Plasma dynamics of water breakdown at a water surface induced by femtosecond laser pulses

C. Sarpe-Tudoran, A. Assion, M. Wollenhaupt, M. Winter, and T. Baumert[a)]
Institute of Physics and Center for Interdisciplinary Nanostructure Science and Technology (CINSaT), University of Kassel, Heinrich-Plett-Strasse 40, D-34132 Kassel, Germany

(Received 23 February 2006; accepted 11 May 2006; published online 29 June 2006)

Femtosecond laser pulse induced ultrafast plasma dynamics studies of water breakdown in the range up to 250 ps are reported. We combine transient imaging techniques together with spectrally resolved reflection spectroscopy to monitor the early breakdown dynamics at the water surface with a laser intensity being 1.5 above threshold. We observe a 20 ps delay before the plasma expands with an initial velocity of 5900 m/s. The transient electron density after formation of the plasma is $1.2\times10^{21}/\mathrm{cm}^3$. A recombination on a picosecond time scale with a rate of $(1.6\times10^{-9}\pm0.3\times10^{-9})$ cm^3/s is found. © *2006 American Institute of Physics*. [DOI: 10.1063/1.2217158]

Laser induced breakdown (LIB) in water has been investigated extensively throughout the last decades due to its numerous applications in precise ablation of biological tissue, therapeutic laser medicine, and chemical analysis.[1] Motivation for these studies stems from the observation that ultrashort laser pulses in the visible and near IR spectral regions interacting with transparent media lead to a decrease of the breakdown threshold with decreasing laser pulse duration.[2–5] This results in deterministic structures with a significant reduction of collateral damage. In water the importance of recombination for picosecond and nanosecond laser induced breakdown has been highlighted[6] and processes after the breakdown event such as cavitations, shock wave propagation, and plasma plume expansion have been studied with femtosecond, picosecond, and nanosecond laser pulses.[7,8] Schaffer *et al.*[9] resolved the plasma dynamics on a very large time scale. However, the breakdown plasma dynamics below 20 ps has not been accurately resolved and plasma parameters such as transient electron density and expansion velocity—important for a better understanding and optimization of the breakdown event—have not been measured directly.

We used a combination of transient imaging techniques together with spectrally resolved reflection spectroscopy to monitor the early breakdown plasma dynamics. We observed that the optical properties of the breakdown plasma created by femtosecond laser pulses on a water surface are quite similar to that of a Fabry-Perot interferometer with a time varying separation. Therefore changes of the plasma thickness in the nanometer range were resolved which allowed to observe the initial expansion dynamics of the plasma and extract important transient plasma parameters.

The investigations were performed in a collinear pump-probe setup at a repetition rate of 1 kHz. An intense femtosecond laser pump pulse and a weak femtosecond probe pulse both of 35 fs duration at 790 nm were focused by a 50 mm lens at normal incidence onto the surface of an interferometrically stable, flat water jet. Because we set the beam waist of the probe laser to be much larger than the plasma distribution, the intensity of the probe laser is constant in the region of the plasma. An infinity corrected objective, a lens, and a beam splitter were used to image the reflected part of the probe laser onto a charge-coupled device (CCD) camera and a pinhole in front of a spectrometer. By using an appropriate pinhole only the reflectivity of the central part of the plasma area was imaged on the spectrometer entrance and used for the spectral recordings. In this way the local reflectivity was measured within a spectral range of 60 nm around 790 nm with a signal to noise ratio higher than 20:1. The spatial and spectral resolutions of the setup are 3 μm and 0.2 nm, respectively. The pump laser intensity used in our measurements was 1.5 times higher than the LIB threshold, defined by a 5% increase of the probe reflectivity within the first picosecond from the pure water jet reflectivity $R_{\mathrm{jet}}=3.9\%$. The measured reflectivity is given by $R(\lambda)=R_{\mathrm{jet}}S_{\mathrm{pl}}(\lambda)/S_{\mathrm{jet}}(\lambda)$, where $S_{\mathrm{jet}}(\lambda)$ and $S_{\mathrm{pl}}(\lambda)$ are the spectra of the probe laser reflected by the unperturbed water jet and the plasma, respectively. Due to the high stability of the water jet, spectral interferences (SIs) caused by the reflection of the probe laser on the front and rear boundaries of the water jet are resolved in S_{jet} and S_{pl} (see Fig. 1). From the SI in S_{jet} at −5 ps a jet thickness of 94.5 μm is derived. The generation

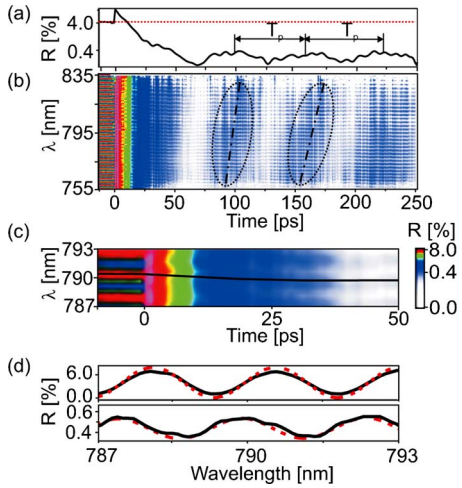

FIG. 1. (Color online) Logarithmic representation of the wavelength integrated reflectivity R (a) and spectrally resolved reflectivity (b) from the center of the breakdown plasma. The dotted line in (a) corresponds to the reflectivity of the pure water jet. Reflectivity oscillation maxima in (b) are indicated by superimposed ellipses to guide the eye. An enlarged section of (b) is shown in (c) and the corresponding spectral interference fringes in (d) at delay times of −5 ps (upper) and 40 ps (lower).

[a)]Author to whom correspondence should be addressed; electronic mail: baumert@physik.uni-kassel.de

of the plasma will finally produce a smaller optical thickness of the jet resulting in a phase shift of the SI [see black line in Fig. 1(c)] similar to the effects of an electron-hole plasma in dielectrics.[10] Analyzing $R(\lambda)$ at −5 and 40 ps [see Fig. 1(d)] we found a decrease in the time delay of the two reflected pulses by (0.7 ± 0.01) fs.

The transient spectra of $R(\lambda)$ from −10 to 250 ps are shown in Fig. 1(b). Each spectrum is recorded with an integration time corresponding to 500 laser shots. The plasma is formed within the duration of the pump pulse which leads to the initial rapid increase of $R(\lambda)$. The wavelength integrated reflectivity shown in Fig. 1(a) decreases within the first 10 ps below R_{jet}. After 30 ps the reflectivity exhibits pronounced oscillations with an averaged period of around 60 ps. The wavelength dependence of the oscillation period in Fig. 1(b) is indicated by the tilt of the superimposed ellipses. These oscillations can be explained if we consider the plasma as an expanding optical thin layer. The two boundaries of the plasma layer (air-plasma and plasma-water) create a Fabry-Perot interferometer producing interferences which are dependent on the phase difference between the light reflected at the front and the rear surfaces of the plasma layer. A complete oscillation of $R(\lambda)$ corresponds to an increase of the optical path within the plasma $n_{\text{pl}}d_{\text{pl}}$ by $\lambda/2$ which will produce frequency dependent oscillation periods, where n_{pl} is the average refraction index of the plasma layer with thickness d_{pl}. As the plasma thickness will increase in time, the tilt angle of the ellipses corresponding to the interference maxima will also increase. Because of the small tilt (0.15 ps/nm) observed for the ellipse corresponding to the first maximum, we can conclude that the initial plasma thickness is in the order of λ.

Guided by these observations we employed a two layer model in order to extract transient plasma parameters especially around the observed strong decrease of the reflectivity within the first 10 ps. This model is based on the generalized Lorentz-Drude dielectric function $\varepsilon(\omega)=\varepsilon_{10}-\omega_{\text{pl}}^2/(\omega^2+i\omega\nu_{\text{el}})$, which is generally used to describe the optical properties of laser produced plasmas, where ε_{10} describes the contribution of bound electrons and its frequency dependence can be neglected. The frequency dependent part of ε is given by the second term, where $\omega_{\text{pl}}=\sqrt{N_e e^2/(m_e\varepsilon_0)}$ is the plasma frequency (which depends on the free electron density N_e) and ν_{el} is the electron-molecule collision frequency. The absorption coefficient κ and the refraction index n_{pl} of the plasma are calculated from $\kappa=\text{Im}(\sqrt{\varepsilon})$ and $n_{\text{pl}}=\text{Re}(\sqrt{\varepsilon})$. By taking into account multiple beam interferences the following expression of the reflectivity is derived:[11]

$$R_{1(2)}(\lambda)=\frac{|r_{1(2)}|^2+2|r_1||r_2|e^{-\beta n_{\text{pl}}d_{\text{pl}}}\cos(\delta+\phi_2-\phi_1)+[|r_{2(1)}|e^{-\beta n_{\text{pl}}d_{\text{pl}}}]^2}{1+2|r_1||r_2|e^{-\beta n_{\text{pl}}d_{\text{pl}}}\cos(\delta+\phi_1+\phi_2)+(|r_1||r_2|e^{-\beta n_{\text{pl}}d_{\text{pl}}})^2}. \quad (1)$$

The index 1 (2) terms the reflectivity from the front (rear) side of the plasma. $\beta=4\pi\kappa/\lambda$ is the linear absorption coefficient and $r_{1(2)}=|r_{1(2)}|e^{i\phi_{1(2)}}$ is the complex reflection factor of the front (rear) surface of the plasma which is calculated by means of the Fresnel equations explicitly given in Ref. 11. In order to analyze the reflectivity data the SI were eliminated by Fourier filtering. The overall reflectivity is given by

$$R(\lambda)=\sigma_1 R_1(\lambda)+\sigma_2[1-R_1(\lambda)]R_w[1-R_2(\lambda)]. \quad (2)$$

The first term describes the contribution of the probe pulse reflected from the plasma whereas the contribution transmitted through the plasma and reflected from the rear side of the jet is described by the second term. The factors $\sigma_1(\sigma_2)$ account for the attenuation of the reflected (transmitted) probe laser caused by scattering and diffraction. R_w is the reflectivity of the water/air boundary. The Fourier filtered spectrally resolved reflectivity data are fitted with $R(\lambda)$ from Eq. (2) in the spectral range of 765–825 nm. Because ω_{pl}^2 is proportional to the electron density N_e, $R(\lambda)$ is a function of σ_1, σ_2, N_e, d_{pl}, ε_{10}, ν_{el}, and n_2, where n_2 is the refraction index of the medium after the second boundary. In this first approach the axial dependence of N_e is neglected and therefore N_e is an average over the axial coordinate. This "step density" model is often used in this kind of problems.[12] The fitting procedure minimizes the standard deviation of the calculated $R(\lambda)$ from the measured one by scanning the fitting parameters in a reasonable large parameter space and leads to the following results. Up to 120 ps the plasma parameter ν_{el} is approximately 1.2/fs. The mean time between momentum transfer $1/\nu_{\text{el}}$ of 0.83 fs agrees with estimations of 1 fs performed by Bloembergen.[13] The attenuation parameter σ_1 fluctuates around 0.95 ± 0.05, whereas σ_2 decreases from 0.98 to below 0.01 in the first 30 ps after plasma formation. Hence a strong diffraction or scattering center is formed. The appearance of a strong scattering center within the first 30 ps was also observed by scattering experiments in transmission geometry.[9] Also, theoretical simulations performed for solid samples suggested that scattering centers will appear on a comparable time scale.[14] The initial value of n_2 agrees with the water value of around 1.3. After 30 ps, n_2 stays below 1.2, which can be a result of thermal processes in water after the second boundary of the plasma layer. In Fig. 2 the transient electron density and the plasma thickness are shown for the first 120 ps. The value of the electron density after the plasma formation is $1.2\times10^{21}/\text{cm}^3$ and remains nearly constant for around 7 ps. After 7 ps the electron density starts to decrease and after 20 ps its value is below $10^{20}/\text{cm}^3$. Because electron diffusion can be neglected on a picosecond time scale[6] we conclude that recombination leads to the observed decrease of the electron density. The generic form of the recombination equation is $dN_e/dt=-\gamma N_e^2$, where γ is the recombination rate. This equation was used to fit the transient electron density in a range from 8 to 26 ps [see the linearized representation in the inset of Fig. 2(b)] and resulted in $\gamma=(1.6\times10^{-9}\pm0.3\times10^{-9})$ cm^3/s. This value is in reasonable agreement with the value of 2.1×10^{-9} cm^3/s obtained from LIB

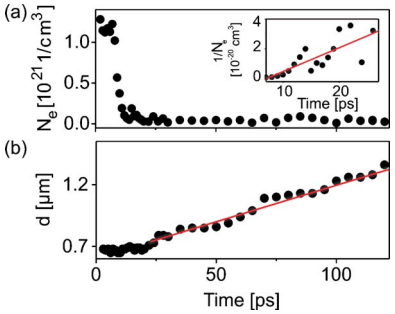

FIG. 2. (Color online) Transient electron density N_e (a) and plasma thickness d (b) obtained from the fit of spectrally resolved reflectivity. A recombination rate of $(1.6\times10^{-9}\pm0.3\times10^{-9})$ cm^3/s [the inset in (a) shows the linearized representation] and an initial expansion velocity of 5900 m/s [straight line in (b)] were obtained.

plasma luminescence studies after excitation with 30 ps laser pulses.[15] The value of the initial electron density is in agreement with recent results reviewed in Ref. 16. The initial plasma thickness value is 0.66 μm and does not change within the first 20 ps. Ablation depth values in fused silica under comparable conditions[17,18] and on plant cells[19] are also in the hundred nanometer regime. Although fused silica and water are different materials, the mechanism of femtosecond LIB is quite similar.[20] The same delay for the plasma expansion process was seen in time resolved scattering experiments in bulk liquid at intensities ten times above threshold.[9] With an electron density of about 10^{21}/cm^3, the initial plasma can be described as supercritical ionized water far from thermodynamic equilibrium. When sufficient kinetic energy from the hot electron gas is transferred to the ions and molecules the plasma starts to expand. From the transient plasma thickness d_{pl} we are able to calculate directly the initial plasma expansion velocity at the water/air interface. The observed plasma velocity is 5900 m/s.

In order to confirm the two layer model the transient spatial distribution of the plasma reflectivity was measured with a CCD camera[21] and the results are compared with the reflectivity calculated from the derived parameters. The measured sections of the reflectivity distribution $R(\lambda)$ along the radial coordinate r for various time delays are shown in Fig. 3(a). The pronounced modulation for $|r|>10$ μm resembles the diffraction pattern of a circular aperture and is caused by the spatial shape of the refraction index distribution in the interaction region. This modulation shows no significant time dependence. However, for $|r|<10$ μm a strong temporal dependence is observed. $R(r)$ not only decreases in time but also changes its profile. In order to understand this behavior $R(r)$ was calculated by means of the two layer model. The lateral electron distribution is described by a Gaussian distribution, where the electron density at the center of the plasma for a given time delay t was taken from the fit of the spectral data. From Fig. 3(b), we see that $R(r)$ for $|r|<10$ μm is reproduced by the calculations (see, for example, the double minimum structure below 9 ps). Hence, all the main features of the spatial distribution $R(r,t)$ within the first 90 ps can be explained by multiple beam interferences on the LIB plasma/vapor layer. This comparison shows consistency between the spatial and spectral experimental approaches reported here.

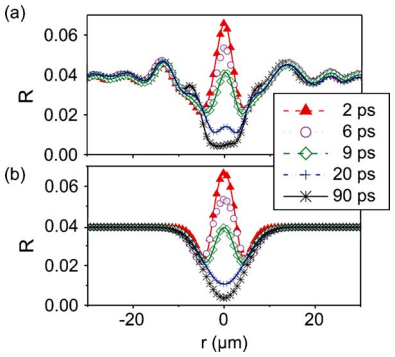

FIG. 3. (Color online) Reflectivity R of the plasma as a function of the lateral coordinate r for different time delays as indicated in the legend: (a) measured and (b) calculated from the derived electron density.

In conclusion, we have investigated laser induced breakdown on a water surface produced by 35 fs laser pulses using transient imaging techniques and spectrally resolved reflection spectroscopy. Our investigations show a 20 ps delay before the plasma expands with an initial expansion velocity of 5900 m/s for laser intensities being 1.5 times above the LIB threshold. Moreover, by analyzing the plasma spectral signature the transient electron density was obtained. After formation of the plasma we determined a value of 1.2×10^{21}/cm^3 and we found that it decreases on a picosecond time scale due to recombination with a rate of $(1.6\times10^{-9}\pm0.3\times10^{-9})$ cm^3/s. Future work will concentrate on higher excitation energies and solid samples.

Financial support of this work by the DFG is gratefully acknowledged.

[1] A. Vogel and V. Venugopalan, Chem. Rev. (Washington, D.C.) **103**, 577 (2003).
[2] B. C. Stuart, M. D. Feit, S. Herman, A. M. Rubenchik, B. W. Shore, and M. D. Perry, Phys. Rev. B **53**, 1749 (1996).
[3] M. Lenzner, J. Krüger, S. Sartania, Z. Cheng, Ch. Spielmann, G. Mourou, W. Kautek, and F. Krausz, Phys. Rev. Lett. **80**, 4076 (1998).
[4] D. Du, X. Liu, G. Korn, J. Squier, and G. Mourou, Appl. Phys. Lett. **64**, 3071 (1994).
[5] B. Rethfeld, Phys. Rev. Lett. **92**, 187401 (2004).
[6] J. Noack and A. Vogel, IEEE J. Quantum Electron. **35**, 1156 (1999).
[7] E. Abraham, K. Minoshima, and H. Matsumoto, Opt. Commun. **176**, 441 (2000).
[8] A. Vogel, S. Busch, and U. Parlitz, J. Acoust. Soc. Am. **100**, 148 (1996).
[9] C. B. Schaffer, N. Nishimura, E. N. Glezer, A. M. T. Kim, and E. Mazur, Opt. Express **10**, 196 (2002).
[10] S. S. Mao, F. Quéré, S. Guizard, X. Mao, R. E. Russo, G. Petite, and P. Martin, Appl. Phys. A: Mater. Sci. Process. **79**, 1695 (2004).
[11] M. Born and E. Wolf, *Principles of Optics-Electromagnetic Theory of Propagation, Interference and Diffraction of Light* (Cambridge University Press, Cambridge, 1999).
[12] W. Theobald, R. Häßner, R. Kingham, R. Sauerbrey, R. Fehr, D. O. Gericke, M. Schlanges, W.-D. Kraeft, and K. Ishikawa, Phys. Rev. E **59**, 3544 (1999).
[13] N. Bloembergen, IEEE J. Quantum Electron. **QE-10**, 375 (1974).
[14] D. Perez and L. J. Lewis, Phys. Rev. B **67**, 184102 (2003).
[15] F. Docchio, Europhys. Lett. **6**, 407 (1988).
[16] A. Vogel, J. Noack, G. Hüttman, and G. Paltauf, Appl. Phys. B: Lasers Opt. **81**, 1015 (2005).
[17] I. H. Chowdhury, X. Xu, and A. M. Weiner, Appl. Phys. Lett. **86**, 151110 (2005).
[18] T. Q. Jia, Z. Z. Xu, X. X. Li, R. X. Li, B. Shuai, and F. L. Zhao, Appl. Phys. Lett. **82**, 4382 (2003).
[19] A. Assion, M. Wollenhaupt, L. Haag, F. Mayorov, C. Sarpe-Tudoran, M. Winter, U. Kutschera, and T. Baumert, Appl. Phys. B: Lasers Opt. **77**, 391 (2003).
[20] M. D. Feit, A. M. Komashko, and A. M. Rubenchik, Appl. Phys. A: Mater. Sci. Process. **79**, 1657 (2004).
[21] K. Sokolowski-Tinten, J. Bialkowski, A. Cavalleri, and D. von der Linde, Appl. Surf. Sci. **127–129**, 755 (1998).